Human Molecular Genetics, 1998, Vol. 7, No. 13 **2029–2037**

ARTICLE

LIS1 and *XLIS* (*DCX*) mutations cause most classical lissencephaly, but different patterns of malformation

Daniela T. Pilz, Naomichi Matsumoto, Sharon Minnerath[1], Patti Mills, Joseph G. Gleeson[4,5], Kristin M. Allen[5], Christopher A. Walsh[5], A. James Barkovich[6], William B. Dobyns[1,2,3,+], David H. Ledbetter[*,+] and M. Elizabeth Ross[1,3,+]

Department of Human Genetics, University of Chicago, 924 East 57th Street, R113, Chicago, IL 60637, USA, [1]Department of Neurology, [2]Department of Pediatrics and [3]Institute of Human Genetics, University of Minnesota Medical School, Minneapolis, MN 44544, USA, [4]Department of Neurology, Children's Hospital, Boston, MA 02115, USA, [5]Division of Neurogenetics, Department of Neurology, Beth Israel Deaconess Medical Center, Harvard Medical School, Boston, MA 02115, USA and [6]Departments of Radiology (Neuroradiology), Neurology and Pediatrics, University of California, San Francisco, CA 94143, USA

Received September 9, 1998; Revised and Accepted September 18, 1998

Classical lissencephaly (LIS) is a neuronal migration disorder resulting in brain malformation, epilepsy and mental retardation. Deletions or mutations of *LIS1* on 17p13.3 and mutations in *XLIS* (*DCX*) on Xq22.3–q23 produce LIS. Direct DNA sequencing of *LIS1* and *XLIS* was performed in 25 children with sporadic LIS and no deletion of *LIS1* by fluorescence *in situ* hybridization. Mutations of *LIS1* were found by sequencing (*n* = 8) and Southern blot (*n* = 2) in a total of 10 patients (40%) of both sexes and mutations of *XLIS* in five males (20%). Combined with previous data, deletions or mutations of these two genes account for ~76% of isolated LIS. These data demonstrate that *LIS1* and *XLIS* mutations cause the majority of, though not all, human LIS. The mutations in *LIS1* were predicted to result in protein truncation in six of eight patients and splice site mutations in two, all of which disrupt one or more of the seven WD40 repeats contained in the *LIS1* protein. Point mutations in *XLIS* identified the C-terminal serine/proline-rich region as potentially important for protein function. The patients with mutations were included in a genotype–phenotype analysis of 32 subjects with deletions or other mutations of these two genes. Whereas the brain malformation due to *LIS1* mutations was more severe over the parietal and occipital regions, *XLIS* mutations produced the reverse gradient, which was more severe over the frontal cortex. The distinct LIS patterns suggest that *LIS1* and *XLIS* may be part of overlapping, but distinct, signaling pathways that promote neuronal migration.

INTRODUCTION

Neuronal heterotopia resulting from impaired neuronal migration has increasingly been implicated as a major cause of 'idiopathic' seizures, possibly accounting for one quarter of pediatric and adult epilepsy (1). Many malformation syndromes with deficient neuronal migration have been described (2). Several of these are associated with classical lissencephaly (LIS) or 'smooth brain', which shows widespread evidence of incomplete neuronal migration. The spectrum of LIS ranges from absent (agyria) or abnormally broad (pachygyria) convolutions to a less severe malformation known as subcortical band heterotopia (SBH). In SBH, bilateral and symmetric ribbons of gray matter are located in the central white matter (3–6). Studies of the gene mutations underlying these disorders will allow discovery of the basic mechanisms responsible for normal neuronal movement during brain development. Not only will this provide a better understanding of these uncommon disorders, but also of the more common isolated heterotopias, hypothesized to result from localized functional impairment of the same or related genes.

Two genes associated with LIS have recently been cloned: *LIS1* and *XLIS* (also known as *DCX*). *LIS1* maps to chromosome 17p13.3 and encodes the β subunit of platelet activating factor acetylhydrolase, brain isoform Ib (βLIS1) (7–13). The gene name has therefore recently been modified to *PAFAH1B1*. *XLIS* is located on Xq22.3–q23 and encodes a protein named doublecortin (14–18). We hypothesize that several other LIS genes must exist based on both human and animal studies (2,19–22).

*To whom correspondence should be addressed. Tel: +1 773 834 0525; Fax: +1 773 834 0505; Email: dhl@genetics.uchicago.edu
+These authors contributed equally to this work

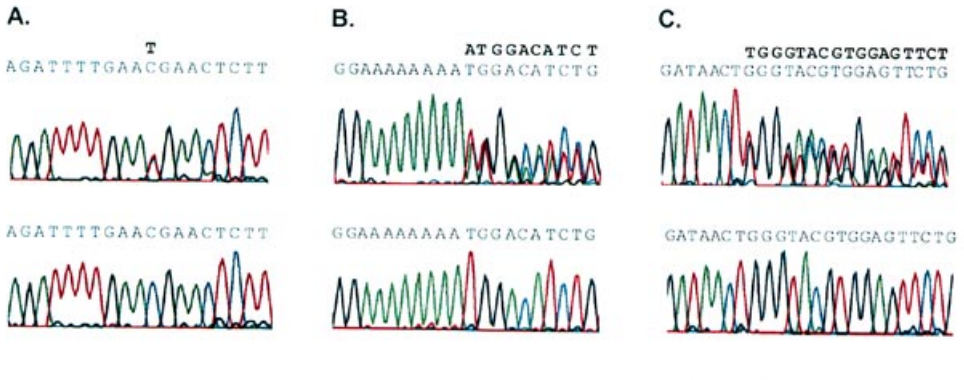

Figure 1. *LIS1* sequence electropherograms of three patients (LP97-078, LP97-068 and LP90-014) with the normal control sequence below in each case. The sequencing changes in the patients are indicated in bold above the normal sequence. (**A**) A C→T change in exon 6 resulting in a stop codon; (**B**) insertion of an A in a poly(A) stretch in exon 4 causes a frameshift and a stop codon downstream; (**C**) insertion of a T in exon 10 also causes a frameshift and a stop codon downstream. The mutations in one of these cases (C) and the patient, whose sequence is shown in Figure 3A, had previously been missed by SSCP screening (7).

Deletions and mutations of *LIS1* have been observed in Miller–Dieker syndrome (MDS) and isolated lissencephaly sequence (ILS), both of which are associated only with LIS (7,23–25), whereas mutations of *XLIS* have been observed in both ILS and SBH, with ILS observed primarily in males and SBH primarily in females (3,14–17). A recent study of 11 females with SBH (also known as subcortical laminar heterotopia or SCLH) found *XLIS* mutations in 10 cases (26).

With the current *LIS1*-specific fluorescence *in situ* hybridization (FISH) probes, deletions of this gene can be detected in 40% of patients with sporadic ILS (23). In this study, comprehensive mutation analysis of *LIS1* and *XLIS* was performed in 25 patients with sporadic ILS in whom no deletion of the *LIS1* region in 17p13.3 was detected by FISH. *XLIS* mutation analysis has not previously been undertaken in males or females with non-familial ILS. Genotype–phenotype analysis was carried out in 32 subjects with ILS and known deletions or other mutations of *LIS1* or *XLIS*, including the 15 patients in whom mutations were detected in this study. The results: (i) demonstrate that the majority of human LIS is caused by these two genes; (ii) indicate putative critical functional domains of the *LIS1* and *XLIS* protein products; and (iii) identify differences in the phenotype between subjects with mutations of the two genes, especially in the gyral pattern, which suggest different roles in neuronal migration.

RESULTS

Mutation analysis (group 1)

LIS1. Mutations in *LIS1* were found in 8/25 group 1 patients (32%) by direct sequencing, including four males and four females. Examples are shown in Figure 1. All mutations were confirmed on a second blood sample from the proband. Sequencing analysis of the parents demonstrated in each case that the change was *de novo*. Six of eight mutations found (subjects LP90-014, LP91-019, LP97-021, LP97-068, LP97-071 and LP97-078) were predicted to result in a truncated protein (Table 1 and Fig. 2). The remaining two were splice donor site changes. One (LP97-067) was a base pair change at the fifth base of intron 9 which produced an RT–PCR product smaller than the normal control (data not shown). Sequencing of the abnormal product revealed skipping of exon 9. The other (LP90-020) was a CA insertion after the third base in intron 10 resulting in an RT–PCR product slighty larger than the normal control (Fig. 3). This insertion appears to result in a cryptic splice site with 86 additional intronic base pairs present between exons 10 and 11, found on sequencing of the abnormal RT–PCR product.

Table 1. Summary of *LIS1* and *XLIS* mutations

Patient	Gene	Location	DNA sequence change	Type of mutation	Predicted protein
LP97-068	*LIS1*	Exon 4	162insA	Frameshift	Truncated
LP97-078	*LIS1*	Exon 6	430C→T	Nonsense	Truncated
LP97-071	*LIS1*	Exon 8	703delGA	Frameshift	Truncated
LP91-019	*LIS1*	Exon 8	805delA	Frameshift	Truncated
LP97-021	*LIS1*	Exon 9	903insT	Frameshift	Truncated
LP97-067	*LIS1*	Intron 9	1002+5G→A	Splice site	Exon 9 skipped
LP90-014	*LIS1*	Exon 10	1018insT	Frameshift	Truncated
LP90-020	*LIS1*	Intron 10	1159+3insCA	Splice Site	Extra amino acids
LP93-004	*XLIS*	Exon 4	128T→C	Missense	L43S
LP91-072	*XLIS*	Exon 4	304C→A	Missense	R102S
LP97-072	*XLIS*	Intron 5	705+1G→A	Splice site	Exon 5 skipped[a]
LP87-008	*XLIS*	Exon 7	907C→T	Nonsense	Truncated
LP89-004	*XLIS*	Exon 7	907C→T	Nonsense	Truncated

[a]RNA not available for confirmation.

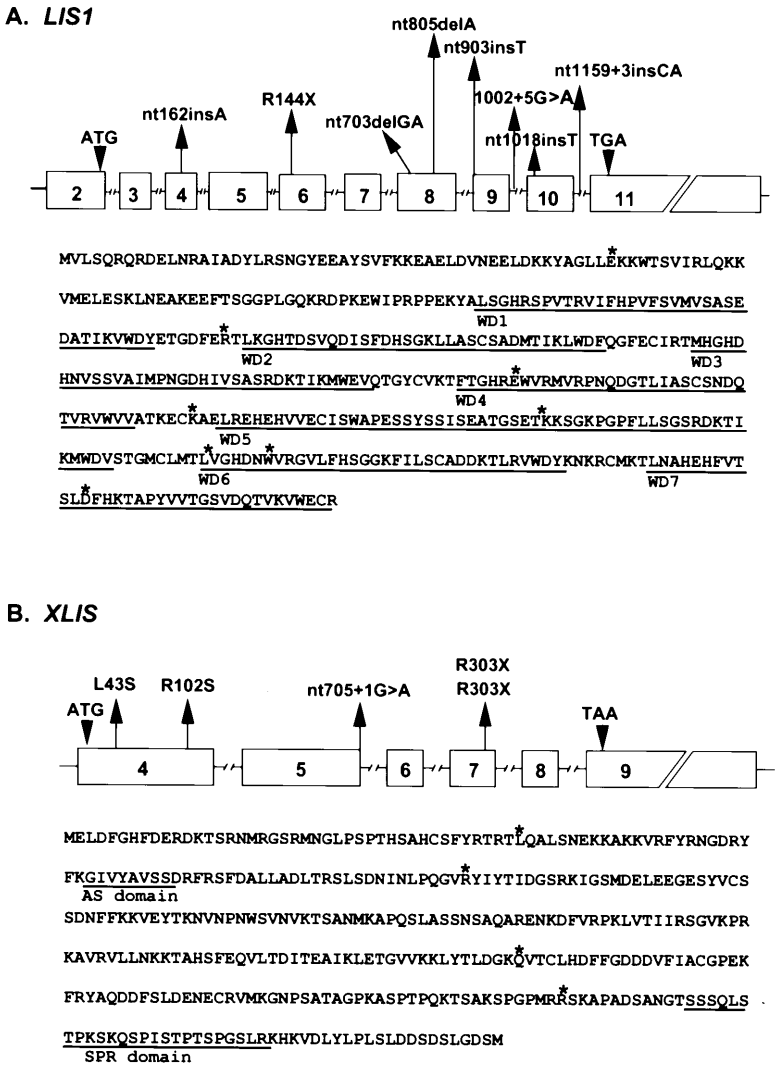

Figure 2. Summary of *LIS1* and *XLIS* mutations in 25 ILS patients. The exon–intron structure of *LIS1* (**A**) and *XLIS* (**B**) and the amino acid sequences of βLIS1 and doublecortin are shown. The locations of the 13 mutations detected are shown in both the gene and protein. The WD40 repeats in βLIS1 and the abl substrate and the serine/proline-rich domain in doublecortin are underlined. nt, nucleotide; WD, WD40 repeat; AS, abl substrate; SPR, serine/proline-rich; *, sequence location of mutations.

Southern blot analysis detected alterations in two additional patients out of four patients in whom sequencing of *LIS1* and *XLIS* had not detected a mutation and who had not previously been studied with this method (see Materials and Methods). In both patients, a *LIS1* rearrangement was detected with three different restriction enzymes (data not shown); parental studies demonstrated that the changes were *de novo*.

XLIS. Mutations in *XLIS* (Table 1 and Fig. 2) were found in five males (5/25 = 20%). Two unrelated males (LP87-008 and LP89-004) had the same nucleotide change (C→T) in exon 7 which led to a premature stop codon at amino acid 303 (Fig. 3). One patient (LP97-072) had a G→A change in intron 5 at the invariant splice donor GT dinucleotide, predicted to lead to abnormal splicing. We were unable to obtain suitable RNA preparations to confirm this. All three mothers of these boys were studied and none of them demonstrated the changes found in their sons; therefore the mutations were *de novo*. Two patients (LP91-072 and LP93-004) had single base pair substitutions that led to an amino acid change. Their mothers have so far been unavailable for study. To exclude the possibility that these changes represent polymorphisms, a PCR–RFLP approach using *Taq*I or *Alu*I, respectively, was utilized (27). The nucleotide changes found in these boys were excluded in 100 normal alleles and it is therefore highly unlikely that these substitutions are polymorphisms.

Genotype–phenotype correlation (group 2)

Different patterns of lissencephaly with LIS1 and XLIS mutations. We found consistent differences on neuroimaging in the antero-posterior malformation gradient of LIS between subjects with mutations of *LIS1* and *XLIS*, with agyria being the most severe and SBH the mildest form of LIS (Table 2). For clarity, we will

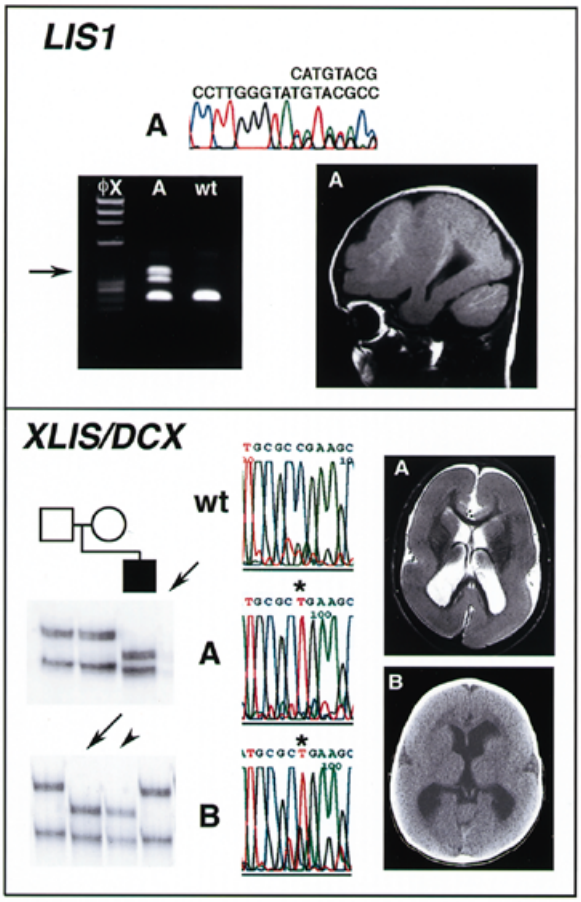

Figure 3. Analysis of mutations in *LIS1* and *XLIS*. (Top) The sequence shows a CA insertion causing a frameshift mutation in intron 10 of *LIS1* found in patient LP90-020 (**A**). The heterozygosity is evident as double peaks on the electropherogram, compared with the single peaks in normal controls. This produces a splice variant, demonstrated by the larger mRNA species detected on RT–PCR of cell lines from patient A (arrow). His MRI reveals LIS grade 3a. (Bottom) An identical *de novo* band shift is shown on SSCP in two unrelated boys: (**A**) LP89-004, arrow; (**B**) LP89-004, arrow, and LP87-008, arrowhead. Sequence electropherograms show a C→T change in exon 7 of *XLIS* in (A) and (B), resulting in a stop codon at residue 303. Images of both boys reveal LIS grade 1b. wt, wild-type control; ΦX, standard size marker.

refer to ILS with mutations of *LIS1* as ILS17 and to ILS with mutations of *XLIS* as ILSX. Those with *LIS1* mutations had more severe LIS over the parietal and occipital regions (P→A; Table 3), whereas subjects with *XLIS* mutations had the reverse gradient with more severe LIS over the frontal regions (A→P; Table 3). This was most evident in those with grades 3 (mixture of agyria and pachygyria) or 4 (generalized or partial pachygyria) LIS (Fig. 4 and Table 3). In addition, mild hypoplasia and upward rotation of the cerebellar vermis was seen in all patients with mutations of *XLIS*, but only in ~20% of patients with *LIS1* mutations (Fig. 4).

Table 2. Grading system for classical LIS and SBH

Grade	Gyral malformations/description
1	Diffuse AGY
2	Diffuse AGY with a few shallow sulci over frontal and temporal (2a) or occipital (2b) poles
3	Mixed AGY and PCH with either frontal PCH and parietooccipital AGY (3a) or parietooccipital PCH and frontal AGY (3b)
4	Diffuse or partial PCH only, which is more severe posteriorly (4a) or frontally (4b)
5	Mixed PCH (posteriorly, 5a; frontally, 5b) and SBH
6	Subcortical band heterotopia (posteriorly, 6a; frontally, 6b)

Modified from Dobyns and Truwit (2). Grades 1–6 denote the overall severity of the LIS malformation as seen on neuroimaging, with grade 1 (generalized agyria) being the most severe and grade 6 (subcortical band heterotopia) the mildest form. Note that grades 1a–6a are more severe posteriorly, especially involving the parietal lobes, while grades 1b–6b are more severe anteriorly, especially involving the anterior and superior frontal lobes. In addition, a normal or simplified gyral pattern over the orbito-frontal regions and to a lesser extent the anterior temporal regions are usually observed with grades 1a–6a, while a normal or simplified gyral pattern over the anterior temporal regions with more severe gyral abnormality of the orbitofrontal regions are usually observed with grades 1b–6b. AGY, agyria; PCH, pachygyria; SBH, subcortical band heterotopia.

Among patients with *LIS1* mutations, there was a spectrum of severity ranging from diffuse agyria (grades 1a and 2a) to frontal pachygyria with parietooccipital agyria (grade 3a) to diffuse pachygyria (grade 4a), all of which were more severe posteriorly. Relative sparing of the orbito-frontal and anterior temporal regions was consistently observed. The severity of LIS varied from grade 1a to 4a in both *LIS1* subgroups (Table 3).

Among patients with *XLIS* mutations, a similar spectrum of severity was observed ranging from diffuse agyria (grades 1b and 2b) to frontal agyria with posterior pachygyria (grade 3b) to diffuse pachygyria (grade 4b), all of which were more severe frontally. Some patients with LIS grade 4b appeared to have almost normal gyri over the occipital region. All had relative sparing of the anterior temporal regions, while the orbito-frontal region was usually abnormal, which differs from children with *LIS1* mutations. Children with sporadic ILSX had more severe LIS than children with familial ILSX. A similar observation has been made in females with sporadic or familial SBH (28).

Mental retardation. The majority of children with ILS17 had profound retardation. There was one exception, a boy with grade 4 LIS, who could walk and use a few short sentences at age 4. He had a *LIS1* splice site mutation leading to skipping of exon 9 and an in-frame deletion of the protein.

All boys with sporadic ILSX had profound retardation and truncating and missense mutations were observed (Table 1). Familial cases had a less severe phenotype; one boy could walk and use limited language. Only missense mutations were found in familial ILSX.

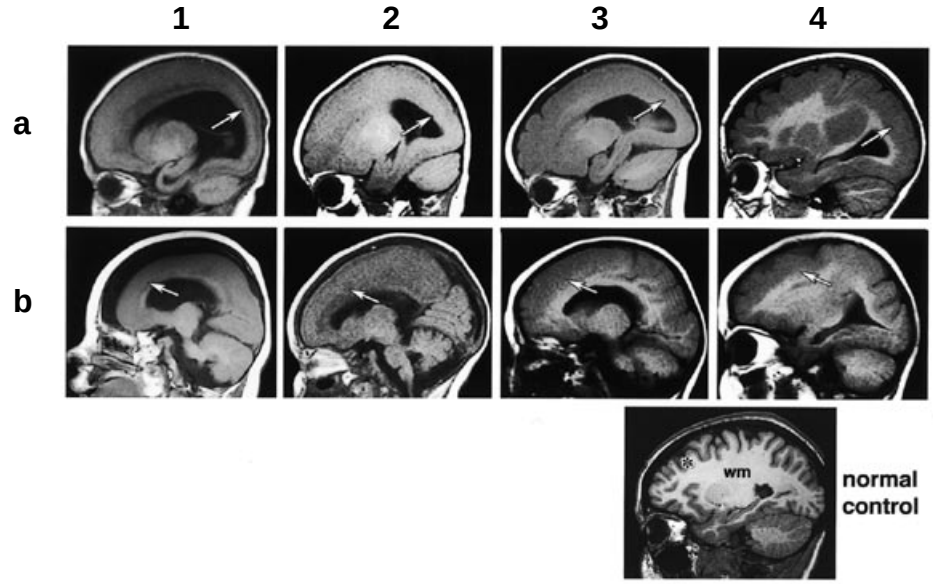

Figure 4. Malformation gradient in LIS due to *LIS1* versus *XLIS* mutation. The scan in the bottom right hand corner shows a normal brain for comparison (*, cortex; wm, white matter). MR images are compared in the sagittal plane: the top row (**a**) is from ILS patients with known mutations of *LIS1*, while the images in the bottom panels (**b**) are from patients with known mutations of *XLIS*. The LIS grades are indicated above (a). Arrows point to regions most severely affected in each scan. Images 1a and 1b are difficult to distinguish. Images 2a and 2b can be distinguished from the emerging sulcal markings indicating pachygyria seen over the frontal pole in 2a and over the occipital pole in 2b. The different gradients become more obvious in comparing 3a with 3b and 4a with 4b. The gyral malformation is more severe over posterior brain regions in 3a and 4a, while the reverse is true in 3b and 4b, with more severe gyral malformations over the frontal regions. These images were selected from patients LP95-059 (1a), LP97-068 (2a), LP95-132 (3a), LP93-005 (4a), LP97-072 (1b), LP97-079 (2b) and LP97-034a1 (used for both 3b and 4b for demonstration purposes, although the scan was rated as 4b).

Table 3. Analysis of lissencephaly in 32 subjects with *LIS1* or *XLIS* mutations

Diagnosis and mutation	*n*	LIS grade 1 or 2		LIS gradient P→A		A→P		Vermis rotation	
		n	%	*n*	%	*n*	%	*n*	%
LIS1 syndromes									
ILS17 (deletion by FISH)	10	3	30	9	90	0	0	2/10	20
ILS17 (intragenic mutation)	12	3	33	12	100	0	0	2/9	22
Total	22	6	27	21	95	0	0	4/19	21
XLIS syndromes									
ILSX (familial)	4	0	0	0	0	4	100	3/3	100
ILSX (sporadic)	6	5	83	0	0	2	33	3/3	100
Total	10	5	50	0	0	6	60	6/6	100

Diagnosis and mutation separates the subjects by type of mutation. Note that the 10 subjects with *LIS1* mutations and the five subjects with *XLIS* mutations from group 1 are included in the ILS17 (intragenic mutations) and ILSX (sporadic) groups.
LIS grade indicates the number and percent of subjects with LIS grades 1 or 2 compared with the total with grades 1–4. Criteria for LIS grades are shown in Table 1.
LIS gradient P→A is the number and percent of subjects in whom the gyral malformation is more severe over posterior compared with anterior brain regions, while A→P indicates the reverse gradient. In five subjects with severe grade 1 LIS, no clear gradient could be determined, sometimes due to suboptimal imaging studies.
Vermis rotation indicates subjects in which the cerebellar vermis was mildly hypoplastic and rotated slightly upward leaving an enlarged foramen of Magendie.

DISCUSSION

LIS1 and *XLIS* mutations account for a majority of ILS

The most common mutation causing LIS is complete deletion of *LIS1*, which has been observed in all patients with MDS and ~40% of those with ILS (23). Mutation analysis of *LIS1* in 25 non-deletion cases with sporadic LIS revealed mutations in a further 10 (40%). Among these, eight were detected by sequencing, three of which were previously missed by SSCP (7; Figs 1 and 3). This confirms that direct DNA sequencing is the most sensitive method for comprehensive mutation analysis. Two mutations were found by Southern blot analysis.

The high percentage of *XLIS* mutations among sporadic ILS males not deleted for *LIS1* (5/13 males = 38%) was striking; it has highlighted the importance of this gene in the etiology of LIS in males. Sequencing of *LIS1* and *XLIS* provided the opportunity to clearly estimate the frequency of mutations in these genes in patients with sporadic ILS who have not been found to have a *LIS1* deletion using gene-specific FISH probes. Mutations of *LIS1* or *XLIS* were found in 15 of 25 non-deletion patients (60%) in the present study. Combined with the previously observed frequency of *LIS1* mutations detected by FISH, these two genes account for ~76% of sporadic ILS.

Functional domains of βLIS1 and doublecortin proteins

Complete or partial deletions of *LIS1* result in loss of function of the involved allele. The *LIS1* protein (βLIS1) contains seven WD40 repeats (Fig. 2A). The WD40 motif is common to the WD repeat superfamily, as seen in G protein β subunits (29). Crystallography of one WD repeat protein showed that the seven repeating units form a circular, propellar-like structure of four β-strands. Proper folding of these regions forms a globular protein that is resistant to proteolysis (29).

Mutations of *LIS1* in our present analysis resulted in a truncated protein in six of eight patients and a splice site mutation in two, all of which disrupted at least one of the seven WD40 repeats. The most 3′ of these was a splice site mutation in intron 10 creating a cryptic splice site downstream, which effectively inactivated only the seventh WD repeat. This patient had grade 3 LIS, indicating that disruption of even one of these WD40 repeats leads to generalized LIS. This is consistent with the extremely high conservation of the *LIS1* protein with only a single amino acid difference between mouse and human (30). All patients studied here had more severe (grades 1–4) LIS and the mutations created a significant disruption of at least one WD40 repeat. We therefore expect that certain missense mutations leading to an amino acid change in a WD40 repeat may be associated with residual protein function and a milder phenotype (LIS grades 5 and 6). So far only one patient with ILS and a missense mutation in *LIS1* has been reported (7) and he had grade 4 LIS.

The *XLIS* gene product, doublecortin, is a cytosolic protein with several potential regions for regulation by phosphorylation and protein interaction (Fig. 2B). The C-terminal end of doublecortin is rich in serine and proline residues, suggesting that serine phosphorylation in the region may be important for doublecortin function. In addition, the proline residues are likely to contribute to the tertiary structure of the protein and hence its functional properties.

Mutations of *XLIS* produce a complete range of LIS grades 1b–6b. Those leading to truncation of doublecortin produced severe LIS. The most C-terminal point mutation observed in this series produced a stop codon at amino acid 303, removing the last 57 of 360 amino acids at the C-terminus of the protein (Fig. 3). As this point mutation results in severe LIS (grade 1b), the C-terminus of doublecortin is predicted to be important for regulation of doublecortin activity or protein stability. Point mutations produced a single amino acid substitution in two of the five males and were found on either side of a putative site of tyrosine phosphorylation by the ABL kinase family (Fig. 2) (15). This implies that the N-terminal region of doublecortin is also important for protein function.

LIS1 and *XLIS* produce inversely related malformation gradients

Prior to cloning of these two genes, differentiation of ILS associated with mutations of *LIS1* and *XLIS* was not possible without a positive family history compatible with X-linked inheritance or detection of a deletion of the *LIS1* region. Identification of the LIS gradient will assist with prediction of the gene involved and thus improve genetic counseling. The different gradients are most obvious with intermediate severity LIS (grades 3 and 4), but are apparent with experience regardless of the severity.

Recognition of the gradients of LIS among patients with *LIS1* versus *XLIS* mutations has implications for the functional relationship between the two protein products. Clearly, the similarities of reduced gyral formation, thickening of the cortical gray matter and relative sparing of cerebellar foliation suggest that *LIS1* and *XLIS* are potentially involved in the same or interacting signal transduction pathways controlling neuronal migration. However, the non-overlapping pattern of increased severity posteriorly with *LIS1* mutations versus anteriorly with *XLIS* mutations raises the possibility that these genes are part of distinct, though related, signaling pathways. This is further supported by observation of the same subtle vermis malformation in a few patients with *LIS1* mutations (Table 3). Northern blot analysis shows *XLIS* to be predominantly expressed in the frontal lobe (31), consistent with the gradient of severity, whereas *LIS1* shows fairly ubiquitous expression in both the frontal and occipital areas of the brain (7).

MATERIALS AND METHODS

Subject selection and clinical review

We selected two overlapping groups of patients with LIS for study. Group 1 consisted of 25 patients (13 males and 12 females) with ILS. Large deletions of *LIS1* were excluded by FISH and 15 of these children had previously been screened for mutations of *LIS1* by SSCP (single strand conformational polymorphism) and Southern blot analysis (7).

Group 2 consisted of 32 patients with ILS in whom deletions or other mutations of *LIS1* or *XLIS* were detected by FISH or sequencing. The 15 patients from group 1 with intragenic mutations of *LIS1* or *XLIS* were included. Results of magnetic resonance images ($n = 28$) or computed tomography scans ($n = 4$) of the brain were obtained for all 32 subjects and were classified using a grading scale modified for this purpose and shown in Table 2. The gradient of LIS was determined by comparing the severity of the gyral malformation over anterior and posterior brain regions. The diagnosis in both groups was confirmed by review of this data in all subjects by the authors (W.B. Dobyns, D.T. Pilz and M.E. Ross). For genotype–phenotype analysis, we subdivided them into four groups including: (i) ILS17 with deletions of *LIS1* detected by FISH; (ii) ILS17 with intragenic mutations of *LIS1*; (iii) sporadic ILSX; and (iv) familial ILSX with intragenic mutations of *XLIS*. Blood samples from probands and often their parents were obtained with informed consent. All protocols were approved by the appropriate Institutional Review Board Human Subjects Committee.

Mutation analysis

DNA and RNA isolation. DNA was extracted from lymphoblast cell lines or peripheral blood using a Puregene DNA isolation kit (Gentra System) according to the manufacturer's protocol. Total RNA was isolated with Trizol (Life Technologies) from lymphoblastoid cell lines of selected patients and of normal controls.

Sequencing. Direct sequencing was performed for the 10 coding exons of *LIS1* and six coding exons of *XLIS* to maximize the mutation detection sensitivity. Genomic DNA was amplified and the PCR products were sequenced by standard protocols using BigDye Primer or BigDye Terminator chemistry (Perkin Elmer). The sequenced products were run on a 4.25% denaturing gel on an ABI 377 automated DNA sequencer (Perkin Elmer). The resulting sequences from the patients and normal controls were aligned and compared with the published sequences deposited in GenBank (*LIS1*, accession nos U72333–U72342; *XLIS*, AF034634 and AJ003112).

LIS1. M13 tailed primers (Table 4) were designed using in part previously published primer sequences (7) for PCR amplification of the patient DNA. PCR products (1 µl) were then directly sequenced in the forward and reverse directions using BigDye Primer chemistry with fluorescent M13 primers (Perkin Elmer). PCR conditions were as follows: 50 µl reaction containing 1× PCR buffer, $MgCl_2$ according to individual primer conditions, 0.2 mM each dNTP, 0.1 µM each primer and 1 U TaqGold polymerase (Perkin Elmer). Thermocycling parameters were: 95°C for 10 min, followed by 10 cycles (20 cycles for exon 9) of 94°C for 45 s, the appropriate annealing temperature for 30 s and 72°C for 1 min, with a further 25 cycles (20 cycles for exon 9) of 94°C for 45 s and 72°C for 1 min.

XLIS. For *XLIS*, several mutations were initially identified by SSCP using conditions as previously described (15). Prior to sequencing (Table 5) with BigDye Terminator chemistry by a standard protocol (Perkin Elmer), the PCR-amplified fragments were purifed using Microcon 100 (Amicon). The PCR was cycled 35 times at 95°C for 30 s, 50°C for 30 s, 72°C for 1 min in a volume of 50 µl containing 1× PCR buffer with 1.5 mM $MgCl_2$, 0.2 mM each dNTP, 1 µM each primer and 2.5 U TaqGold polymerase (Perkin Elmer). Maternal DNA was unavailable for study in two patients. To exclude that the amino acid changes found in these two patients were polymorphisms, 60 unrelated normal controls (20 males and 40 females) were also examined by a PCR–RFLP approach (27). As there were no restriction sites in the variant, a sequence mismatch was introduced in the 3′-region of one of each of the PCR primers creating a new restriction site for *Alu*I or *Taq*I as described (27). The PCR products were digested with *Alu*I or *Taq*I.

Table 4. Primer sequences for PCR amplification of *LIS1*

Primer name	Primer sequence[a]	T_a (°C)	Unique primer sequence product length (bp)
Exon2F-M13	tgtaaaacgacggccagtTGTGGAAGACACTTAGTGGCA	58	269
Exon2R-M13	caggaaacagctatgaccAAGAGACCTCCCAAAGCTGTA	58	
Exon 3F-M13	tgtaaaacgacggccagtAAGAGTATCTTCAGGGTTAATG	58	299
Exon3R-M13	caggaaacagctatgaccTTGTGCGTAACTGTTAACTACA	58	
Exon4F-M13	tgtaaaacgacggccagtTCTTGAGGATCATAGTTAAGCC	56	240
Exon4R-M13	caggaaacagctatgaccTGCAGAAGAATGTTATTTTCAG	56	
Exon5F-M13	tgtaaaacgacggccagtGAAATCTATCTGTACGTAACTAC	58	369
Exon5R2-M13	caggaaacagctatgaccATCTCGGCTCACTGCAAACT	58	
Exon6F-M13	tgtaaaacgacggccagtAAGGAGTGATGGAGTTGGTG	56	336
Exon6R-M13	caggaaacagctatgaccGGGACACTGTACACTGTTAG	56	
Exon7F-M13	tgtaaaacgacggccagtAACCCCATGGTAAAATCCCAT	58	345
Exon7R-M13	caggaaacagctatgaccGGCTGGTCTTCAATTCCTGA	58	
Exon8F-M13	tgtaaaacgacggccagtTTCTGGGAAGTGTCCTGATG	56	368
Exon8R-M13	caggaaacagctatgaccCAGATATCAGCAATAAAACCATG	56	
Exon9F-M13	tgtaaaacgacggccagtGTCCATACCTAACTTTCTTGTG	56	263
Exon9R-M13	caggaaacagctatgaccCATAAAGCATTAATCCCAAAAGG	56	
Exon10F-M13	tgtaaaacgacggccagtGATGCTATTTAAACATTTTGCC	56	302
Exon10R-M13	caggaaacagctatgaccTTTGTCTGGCACTCCAAAATC	56	
Exon11F-M13	tgtaaaacgacggccagtGGTCTCACTATGTTTGTTGTCCA	58	223
Exon11R-M13	caggaaacagctatgaccGGTATCATCAGAGTGCATCCAG	58	

[a]The M13 tails are shown in lower case and the unique sequences of the primers in upper case.

Table 5. Primer sequences for PCR amplification and direct sequencing of *XLIS*

Exon	Primer sequence for PCR	Primer for direct sequencing	PCR product size (bp)
4	Forward 5′-CTTCACCCCCATCCCTTTCT-3′	5′-ATCCCTTTCTCCCACGCT-3′	470
	Reverse 5′-TAACCAATGATGCCACCTCC-3′	5′-ATGCCACCTCCCACCAAC-3′	
5	Forward 5′-TTGGTTAGAATAATCCATATATCTGCT-3′	As PCR primer	514
	Reverse 5′-GGAGGAAGAGTCCGTCAAC-3′	As PCR primer	
6	Forward 5′-GATGATGGCCTAGATGGGAA-3′	5′-GGTTCATTGTCACAGGACCA-3′	278
	Reverse 5′-CAAACCCATGGAAATCCTAAA-3′	5′-GGGAGAGAACAATGGAGCAA-3′	
7	Forward 5′-CATGCTGAGCCTGTTTTATCC-3′	5′-TGTGTCCTTTTGCCCCAG-3′	241
	Reverse 5′-TGTCCTCCATAAATGAAGTCAG-3′	As PCR primer	
8	Forward 5′-TGCTCCTTTGTATGCTGTTGA-3′	As PCR primer	218
	Reverse 5′-AACCTTCACCAAGCCATTCAG-3′	As PCR primer	
9	Forward 5′-AGCAGACATTCCAGAGCTCAA-3′	5′-GGAAAATTAACTTTGTCTCTTCTCTTC-3′	166
	Reverse 5′-GGCTTGGATTTGTACTCTGGA-3′	5′-GACTCTGAGCACTCTCCCCTC-3′	

RNA studies. RNA of the two patients with a *LIS1* splice site mutation and a normal control was reverse transcribed using the Advantage RT for PCR kit (Clontech Laboratories). Transcription was undertaken with both the random hexamer and oligo(dT)$_{18}$ primer. Aliquots of 5 µl cDNA were used for the PCR reaction. Primers were designed for *LIS1* exons 8 and 10 and the 3′-UTR (details available from the authors). PCR conditions: 50 µl reaction containing 1× PCR buffer, 2.5 mM $MgCl_2$, 0.2 mM each dNTP, 0.1 µM each primer and 1 U TaqGold polymerase (Perkin Elmer). The reactions were denatured at 95°C for 10 min, followed by 35 cycles of 94°C for 45 s, 55°C for 30 s and 72°C for 1 min. PCR products were separated on a 4% polyacrylamide gel and the DNA extracted from the aberrant band. The DNA was then sequenced using DyeTerminator chemistry (Perkin Elmer).

Southern blot analysis. Aliquots of 8 µg genomic DNA from the patients and normal controls was digested with restriction enzymes *Eco*RI, *Pst*I, *Bam*HI and *Hin*dIII and separated on a 1% agarose gel. The *LIS1* cDNA clone 47 (8) was digested with *Eco*RI and the insert was used as a probe. Southern transfer, radiolabeling of the cDNA probe, hybridization to Southern blots and washes were performed as previously described (32). An optical scanner (Storm860; Molecular Dynamics) was used to image the blot.

ACKNOWLEDGEMENTS

The authors are greatly indebted to the parents of these children, whose cooperation has been critical to the success of our studies. We would like to thank Stephanie Mewborn and Julie Kuc for their expert technical assistance. This work was supported in part by grants from the National Institutes of Health to M.E.R. and W.B.D. (R01NS35515) and to C.A.W. (NINDS RO1 NS35129) and by the Lissencephaly Network Inc.

REFERENCES

1. Kuzniecky,R. and Jackson,G. (1995) *Magnetic Resonance in Epilepsy*. Raven Press, New York, NY.
2. Dobyns,W.B. and Truwit,C.L. (1995) Lissencephaly and other malformations of cortical development: 1995 update. *Neuropediatrics*, **26**, 132–147.
3. Dobyns,W.B., Andermann,E., Andermann,F., Czapansky-Beilman,D., Dubeau,F., Dulac,O., Guerrini,R., Hirsch,B., Ledbetter,D.H., Lee,N.S., Motte,J., Pinard,J.-M., Radtke,R.A., Ross,M.E., Tampieri,D., Walsh,C.A. and Truwit,C.L. (1996) X-linked malformations of neuronal migration. *Neurology*, **47**, 331–339.
4. Barkovich,A.J., Guerrini,R., Battaglia,G., Kalifa,G., N'Guyen,T., Parmeggiani,A., Santucci,M., Giovanardi-Rossi,P., Granata,T. and D'Incerti,L. (1994) Band heterotopia: correlation of outcome with magnetic resonance imaging parameters. *Ann. Neurol.*, **36**, 609–617.
5. Barkovich,A.J., Koch,T.K. and Carrol,C.L. (1991) The spectrum of lissencephaly: report of ten cases analyzed by magnetic resonance imaging. *Ann. Neurol.*, **30**, 139–146.
6. Crome,L. (1956) Pachygyria. *J. Pathol. Bacteriol.*, **71**, 335–352.
7. Lo Nigro,C., Chong,S.S., Smith,A.C.M., Dobyns,W.B. and Ledbetter,D.H. (1997) Point mutations and an intragenic deletion in LIS1, the lissencephaly causative gene in isolated lissencephaly sequence and Miller–Dieker syndrome. *Hum. Mol. Genet.*, **6**, 157–164.
8. Chong,S.S., Pack,S.D., Roschke,A.V., Tanigami,A., Carrozzo,R., Smith,A.C.M., Dobyns,W.B. and Ledbetter,D.H. (1997) A revision of the lissencephaly and Miller–Dieker syndrome critical regions in chromosome 17p13.3. *Hum. Mol. Genet.*, **6**, 147–155.
9. Ho,Y.S., Swenson,L., Derewenda,U., Serre,L., Wei,Y., Dauter,Z., Hattori,M., Adachi,T., Aoki,J., Arai,H., Inoue,K. and Derewenda,Z.S. (1997) Brain acetylhydrolase that inactivates platelet-activating factor is a G-protein-like trimer. *Nature*, **385**, 89–93.
10. Hattori,M., Adachi,H., Tsujimoto,M., Arai,N. and Inoue,K. (1994) Miller–Dieker lissencephaly gene encodes a subunit of brain platelet-activating factor acetylhydrolase. *Nature*, **370**, 216–218.
11. Reiner,O., Carrozzo,R., Shen,Y., Wehnert,M., Faustinella,F., Dobyns,W.B., Caskey,C.T. and Ledbetter,D.H. (1993) Isolation of a Miller–Dieker lissencephaly gene containing G protein beta-subunit-like repeats. *Nature*, **364**, 717–721.
12. Ledbetter,S.A., Kuwano,A., Dobyns,W.B. and Ledbetter,D.H. (1992) Microdeletions of chromosome 17p13 as a cause of isolated lissencephaly. *Am. J. Hum. Genet.*, **50**, 182–189.
13. Dobyns,W.B., Stratton,R.F., Parke,J.T., Greenberg,F., Nussbaum,R.L. and Ledbetter,D.H. (1983) Miller–Dieker syndrome and monosomy 17p. *J. Pediat.*, **102**, 552–558.

14. des Portes,V., Pinard,J.M., Billuart,P., Vinet,M.C., Koulakoff,A., Carrie,A., Gelot,A., Dupuis,E., Motte,J., Berwald-Netter,Y., Catala,M., Kahn,A., Beldjord,C. and Chelly,J. (1998) A novel CNS gene required for neuronal migration and involved in X-linked subcortical laminar heterotopia and lissencephaly syndrome. *Cell*, **92**, 51–61.
15. Gleeson,J.G., Allen,K.M., Fox,J.W., Lamperti,E.D., Berkovic,S., Scheffer,I., Cooper,E.C., Dobyns,W.B., Minnerath,S.R., Ross,M.E. and Walsh,C.A. (1998) doublecortin, a brain-specific gene mutated in human X-linked lissencephaly and double cortex syndrome, encodes a putative signaling protein. *Cell*, **92**, 63–72.
16. Ross,M.E., Allen,K.M., Srivistava,A.K., Featherstone,T., Gleeson,J.G., Hirsch,B., Harding,B.N., Abdullah,R., Andermann,E., Berg,M., Czapansky-Beilman,D., Flanders,D.J., Guerrini,R., Motté,J., Puche Mira,A., Scheffer,I., Berkovic,S., King,R.A., Ledbetter,D.H., Schlessinger,D., Dobyns,W.B. and Walsh,C.A. (1997) Linkage and physical mapping of X-linked lissencephaly/SBH (XLIS): a gene causing neuronal migration defects in human brain. *Hum. Mol. Genet*., **6**, 555–562.
17. des Portes,V., Pinard,J.M., Smadja,D., Moote,J., Boespflueg-Tanguy,O., Moutard,M.L., Desguerre,I., Billuart,P., Carrie,A., Bienvenu,T., Vinet,M.C., Bachner,L., Beldjord,C., Dulac,O., Kahn,A., Ponsot,G. and Chelly,J. (1997) Dominant X linked subcortical laminar heterotopia and lissencephaly syndrome (XSCLH/LIS): evidence for the occurence of mutation in males and mapping of a potential locus in Xq22. *J. Med. Genet*., **34**, 177–183.
18. Dobyns,W.B., Elias,E.R., Newlin,A.C., Pagon,R.A. and Ledbetter,D.H. (1992) Causal heterogeneity in isolated lissencephaly. *Neurology*, **42**, 1375–1388.
19. Fink,J.M., Hirsch,B.A., Zheng,C., Deitz,G., Hatten,M.E. and Ross,M.E. (1997) Astrotactin, a gene for glial-guided neuronal migration, maps to human chromosome1q25.2. *Genomics*, **40**, 202–205.
20. Ware,M., Fox,J., Gonzalez,J., Davis,N., Lambert de Rouvroit,C., Chua,S., Goffinet,A. and Walsh,C. (1997) Aberrant splicing of a mouse disabled homolog, mdab1, in the scrambler mouse. *Neuron*, **19**, 1–20.
21. Zheng,C., Heintz,N. and Hatten,M.E. (1996) CNS gene encoding astrotactin, which supports neuronal migration along glial fibers. *Science*, **272**, 417–419.
22. Hirotsune,S., Takahara,T., Sasaki,N., Hirose,K., Yoshiki,A., Ohashi,T., Kusakabe,M., Murakami,Y., Watanabe,S., Nakao,K., Katsuki,M. and Hayashizaki,Y. (1995) The reeler gene encodes a protein with an EGF-like motif expressed by pioneer neurons. *Nature Genet*., **10**, 77–83.
23. Pilz,D., Macha,M., Precht,K., Smith,A., Dobyns,W. and Ledbetter,D. (1998) Fluorescence *in situ* hybridization analysis with LIS1 specific probes reveals a high deletion mutation rate in isolated lissencephaly sequence. *Genet. Med*., in press.
24. Dobyns,W.B., Reiner,O., Carrozzo,R. and Ledbetter,D.H. (1993) Lissencephaly: a human brain malformation associated with deletion of the LIS1 gene located at chromosome 17p13. *J. Am. Med. Assoc*., **270**, 2838–2842.
25. Dobyns,W.B., Curry,C.J.R., Hoyme,H.E., Turlington,L. and Ledbetter,D.H. (1991) Clinical and molecular diagnosis of Miller–Dieker syndrome. *Am. J. Hum. Genet*., **48**, 584–594.
26. des Portes,V., Francis,F., Pinard,J.M., Desguerre,I., Moutard,M.L., Snoeck,I., Meiners,L.C., Capron,F., Cusmai,R., Ricci,S., Motte,J., Echenne,B., Ponsot,G., Dulac,O., Chelly,J. and Beldjord,C. (1998) doublecortin is the major gene causing X-linked subcortical laminar heterotopia. *Hum. Mol. Genet*., **7**, 1063–1070.
27. Gotoda,T., Manning,B.S., Goldstone,A.P., Imrie,H., Evans,A.L., Strosberg,A.D., McKeigue,P.M., Scott,J. and Aitman,T.J. (1997) Leptin receptor gene variation and obesity: lack of association in a white British male population. *Hum. Mol. Genet*., **6**, 869–876.
28. Gleeson,J.G., Minnerath,S., Allen,K.M., Fox,J.W., Hong,S., Berg,M., Kuzniecky,R., Reitnauer,P.J., Borgatti,R., Mira,A.P., Guerrini,R., Holmes,G., Rooney,C., Berkovic,S., Scheffer,I., Cooper,E.C., Ricci,S., Cusmai,R., Crawford,T.O., Brown,L., Anderman,E., Wheless,J., Dobyns,W.B., Ross,M.E. and Walsh,C.A. (1999) Characterization of mutations in the gene doublecortin in patients with double cortex syndrome. *Ann Neurology*, in press.
29. Garcia-Higuera,I., Fenoglio,J., Li,Y., Lewis,C., Panchenko,M.P., Reiner,O., Smith,T.F. and Neer,E.J. (1996) Folding of proteins with WD-repeats: comparison of six members of the WD-repeat superfamily to the G protein beta subunit. *Biochemistry*, **35**, 13985–13994.
30. Peterfy,M., Gyuris,T., Basu,R. and Takacs,L. (1994) Lissencephaly-1 is one of the most conserved proteins between mouse and human: a single amino acid difference in 140 residues. *Gene*, **150**, 415–416.
31. Sossey-Alaoui,K., Hartung,A.J., Guerrini,R., Manchester,D.K., Posar,A., Puche-Mira,A., Andermann,E., Dobyns,W.B. and Srivastava,A.K. (1998) Human doublecortin (DCX) and the homologous gene in mouse encode a putative Ca^{2+}-dependent signaling protein which is mutated in human X-linked neuronal migration defects. *Hum. Mol. Genet*., **7**, 1327–1332.
32. Kubota,T., Sutcliffe,J.S., Aradhya,S., Gillessen-Kaesbach,G., Christian,S.L., Horsthemke,B., Beaudet,A.L. and Ledbetter,D.H. (1996) Validation studies of SNRPN methylation as a diagnostic test for Prader–Willi syndrome. *Am. J. Med. Genet*., **66**, 77–80.